Discrete surface solitons in semi-infinite binary waveguide arrays

Mario I. Molina
Departamento de Física, Facultad de Ciencias, Universidad de Chile, Santiago, Chile

Ivan L. Garanovich, Andrey A. Sukhorukov, and Yuri S. Kivshar
Nonlinear Physics Centre and Centre for Ultrahigh-bandwidth Devices for Optical Systems (CUDOS), Research School of Physical Sciences and Engineering, Australian National University, Canberra, ACT 0200, Australia

We analyze discrete surface modes in semi-infinite binary waveguide arrays, which can support simultaneously two types of discrete solitons. We demonstrate that the analysis of linear surface states in such arrays provides important information about the existence of nonlinear surface modes and their properties. We find numerically the families of both discrete surface solitons and nonlinear Tamm (gap) states and study their stability properties.

PACS numbers:

Discreteness effects are known to stabilize surface modes in nonlinear lattices [1, 2], and stable light self-trapping at the edge of a nonlinear self-focusing lattice accompanied by the formation of a discrete surface soliton has recently been demonstrated experimentally [3] Such *unstaggered discrete surface modes* can be treated as discrete solitons trapped at the edge of a waveguide array when the beam power exceeds a certain critical value associated with a strong repulsive surface energy [4].

On the other hand, staggered linear surface modes are known as Tamm states [5], and they were first found in solid state physics as localized electronic states at the edge of a truncated periodic potential; an optical analog of linear Tamm states has been demonstrated for the case of an interface separating periodic and homogeneous dielectric media [6]. ¿From that perspective staggered surface gap solitons in defocusing semi-infinite periodic media, recently introduced theoretically [7] and observed experimentally [8], provide a full analogy to localized electronic surface Tamm states being an optical realization of *nonlinear Tamm states*.

The aim of this Letter is twofold. First, we clarify important links between different types of linear and nonlinear surface modes and demonstrate that the analysis of linear surface states in waveguide arrays with defects provides important information about possible existence of nonlinear surface modes. Second, we study discrete nonlinear surface states in semi-infinite binary waveguide arrays, previously introduced theoretically [9, 10] and then studied experimentally [11], and find numerically the families of both discrete surface solitons and nonlinear Tamm (gap) states and analyze their stability.

We consider propagation and localization of light in a semi-infinite periodic binary array of alternating wide and narrow weakly coupled optical waveguides, as shown schematically in Fig. 1(top). In infinite binary waveguide arrays, the properties of spatial discrete solitons can be effectively managed by controlling the geometry of the array [9, 10, 11]. Following the earlier analysis [9, 10], we describe the binary array within the tight-binding approximation, where the total field is decomposed into a

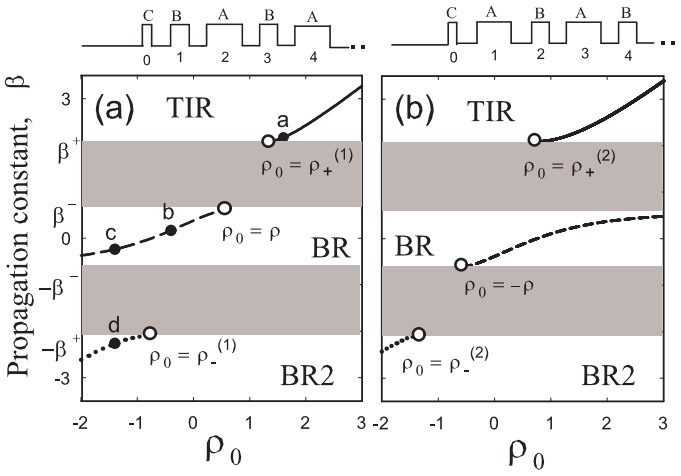

FIG. 1: (a,b) Spectra of the linear surface modes in a binary array of alternating thick (A) and thin (B) optical waveguides with a surface defect (C) for two configurations of a semi-infinite structure shown schematically on top. Shaded areas mark two bands of an infinite binary array ($\rho = 0.6$). Marked points correspond to the examples shown in Figs.2(a-d).

superposition of weakly overlapping modes of the individual waveguides of two kinds (A and B; wide and narrow). The corresponding equation for the mode amplitudes takes the form [9]

$$i\frac{dE_n}{dz} + \rho_n E_n + (E_{n-1} + E_{n+1}) + \gamma_n |E_n|^2 E_n = 0, \quad (1)$$

where $n = 0, 1, \ldots$, and $E_{-1} \equiv 0$ due to the structure termination. Here ρ_n characterizes the linear propagation constant of the mode guided by the $n-$th waveguide, γ_n are the effective nonlinear coefficients (we consider Kerr-type medium response). For the structure shown in Fig. 1(a, top), we have $\rho_{2n+1} = -\rho$, $\rho_{2n} = \rho$, and for Fig. 1(b, top), $\rho_{2n+1} = \rho$, $\rho_{2n} = -\rho$, where $\rho > 0$ defines the difference between the propagation constants of the modes guided by wide and narrow waveguides.

According to Eq. (1), the linear Bloch-wave dispersion is defined as $K_b = \cos^{-1}(-\eta/2)$, where $\eta = 2 + \rho^2 - \beta^2$. The transmission bands correspond to real K_b, and they appear when $\beta_- \le |\beta| \le \beta_+$, where $\beta_- = |\rho|$ and $\beta_+ = (\rho^2+4)^{1/2}$. The band-gap structure is presented in Figs. 1(a,b). The upper gap at $\beta > \beta_+$ is due to the effect of total internal reflection (TIR gap), whereas additional BR and BR2 gaps appear for $|\beta| < \beta_-$ and $\beta < -\beta_+$, respectively, due to Bragg reflection.

In a general case, we assume that the edge waveguide (C) differs from both broad (A) and narrow (B) waveguides, and it is described by a different normalized propagation constant, ρ_0. Then, we study linear surface modes for two possible configurations of the binary array with the defect at the edge [see top insets in Figs. 1(a,b)]. We look for the localized solutions of Eq. (1) at $\gamma_n \equiv 0$ in the form $E_n = u_n \exp(i\beta z)$, where β is the propagation constant and u_n is the mode profile. Such eigenmodes of the semi-infinite periodic structure with a surface defect can be found as truncated Bloch waves of the corresponding infinite structure, where the equation for the edge waveguide defines an effective boundary condition, $\rho_0 = -\rho_1 + [1 + \exp(-iK_b)]/(\beta - \rho_1)$. The mode becomes exponentially localized inside the gaps where the Bloch wave number is complex, and $\mathrm{Im}K_b(\beta) > 0$. Indeed, we find that spatially localized modes can appear in the semi-infinite total internal reflection (TIR) gap [solid curve in Figs. 1(a,b)] or inside the Bragg reflection gaps [dashed and dotted lines in Figs. 1(a,b) correspond to BR and BR2 gaps, respectively].

We find that the surface localized modes may appear in all three gaps of the wave spectra, as shown in Figs. 1(a,b), where the marked values of ρ_o are: $\rho_\pm^{(1)} = (\rho/2) \pm \sqrt{(\rho/2)^2+1}$, for the structure in Fig. 1(a) and $\rho_\pm^{(2)} = -(\rho/2) \pm \sqrt{(\rho/2)^2+1})$, for the structure in Fig. 1(b). Examples of the linear surface modes from different gaps corresponding to the binary array shown in Fig. 1(a) are presented in Figs. 2(a-d).

One of the major observations is that, for the case when there is no surface defect and the binary array is just cut, i.e. $\rho_0 = \rho$ [see Fig. 1(a)] or $\rho_0 = -\rho$ [see Fig. 1(b)], similar to the original formulation of the problem for the Tamm states [5], *no linear localized surface modes* exist in the system, similar to the case of an array composed of identical waveguides discussed earlier [2]. The existence of linear surface modes becomes possible solely due to the presence of a defect located at the edge of the waveguide array, and such localized modes are associated with a specific shift of the beam propagation constant when $\rho_0 \neq \rho$ [Fig. 1(a)] and $\rho_0 \neq -\rho$ [Fig. 1(b)]. The structure of a particular surface mode supported by a defect reflects its location with respect to the photonic bandgap of the binary array: i.e. it is unstaggered in the TIR gap [Fig. 2(a)], staggered in the BR gap [Figs. 2(b,c)], and doubly-staggered in the BR2 gap [Fig. 2(d)].

As is well established in many problems of nonlinear optics, a nonlinear dependence of the optical refractive

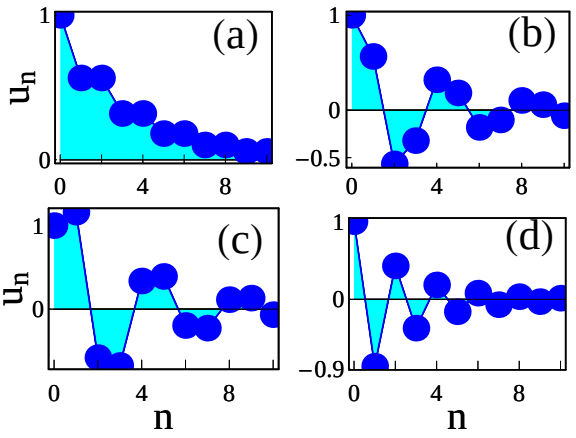

FIG. 2: (Color online) Examples of the linear surface modes in the binary waveguide array shown in Fig. 1(a). The mode profiles in (a), (b), (c) and (d) are associated with different gaps of the linear spectrum and correspond to the points "a", "b", "c" and "d" marked in Fig. 1(a).

index on the intensity of the incoming light provides an important physical mechanism of the intensity-induced shift of the propagation constant which can act as an effective surface defect. Thus, when we consider the case of a nonlinear binary waveguide array, the mode propagation constant becomes shifted by nonlinearity, and for the focusing nonlinear response this shift will be always positive. We analyze below two cases where either a wide or a narrow waveguide is placed at the edge of the array, i.e. when the defect waveguide is created solely by the nonlinearity, similar to the case of nonlinear truncated lattices studied earlier [2]. Just as in the linear case, we look for spatially localized solutions of Eq. 1, now with the nonlinear term (we neglect the differences in the effective nonlinear coefficients at the A and B sites and assume $\gamma_n \equiv 1$), in the form $E_n = u_n \exp(i\beta z)$, where β is the propagation constant, and the function u_n describes the soliton profile.

In Figs. 3 and 4, we show the families of nonlinear surface solitons for two kinds of termination. In the case when the edge waveguide is narrow [Fig. 3], the nonlinear Tamm states (i.e. nonlinear surface modes in the BR gap) appear at low power, in agreement with the linear analysis predicting the existence of surface state for a small change of the propagation constant [dashed curve in Fig. 1(b)]. On the other hand, the existence of the surface mode in the TIR gap requires the mode power to exceed some threshold value, similar to the critical value of the defect strength found in the linear theory [solid curve in Fig. 1(b)]. When the binary lattice is truncated at the wide waveguide [Fig. 4], a finite power is required to support the surface solitons in either TIR or BR gaps, reflecting the properties of linear TIR modes which can be supported only when a positive shift of the propagation constant exceeds a certain threshold value [solid and dashed curves in Fig. 1(a)].

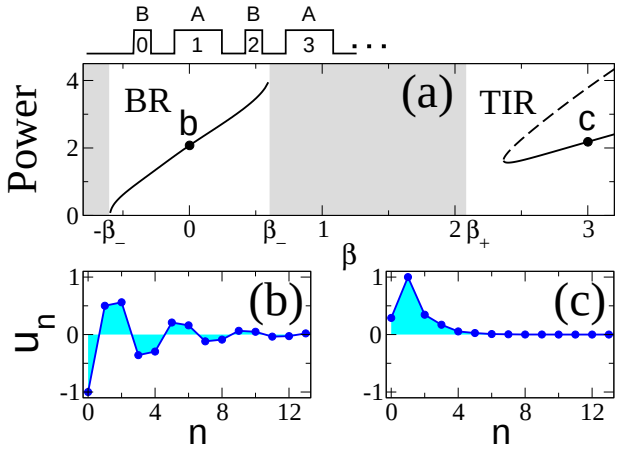

FIG. 3: (Color online) (a) Families of nonlinear Tamm (gap) states and discrete surface solitons in the binary array truncated at the narrow waveguide. Solid and dashed curves correspond to the stable and unstable branches, respectively. Schematic of the array is shown on the top. (b,c) Characteristic examples of the soliton profiles corresponding to the points "b" and "c" marked in (a). Detuning parameter of the array is $\rho = 0.6$.

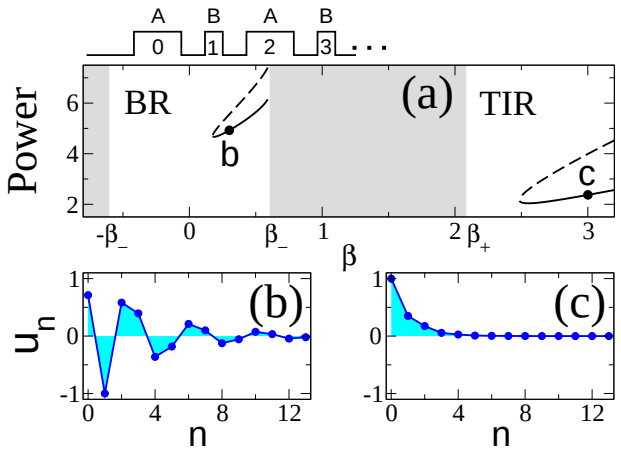

FIG. 4: (Color online) Same as in Fig. 3, but for the binary array truncated at the wide waveguide.

Next, we employ the beam propagation method to study the soliton stability. In Figs. 3(a) and 4(a), dashed branches of the curves indicate unstable surface modes. Whereas oscillatory instabilities [12] may arise for the solid branches, we have verified that the solitons corresponding to the marked points on the solid curves demonstrate stable propagation for more than 100 coupling lengths even in the presence of initial perturbations.

Finally, we mention that the recent studies of discrete gap solitons in binary waveguide arrays provided an experimental evidence [11] of a controlled soliton generation and power-dependent soliton steering in agreement with earlier theoretical predictions [9, 10]. The surface modes in the form of discrete surface solitons and nonlinear Tamm (gap) states described in this paper extend the class of such discrete nonlinear modes, and they can be treated as the discrete solitons trapped at the edge of a waveguide array when the beam power exceeds a certain critical value associated with a strong repulsive surface energy [4]. We believe that our results open a road for the experimental studies of intriguing properties of discrete surface gap solitons in engineered periodic structures.

In conclusion, we have analyzed linear surface states at the edge of a semi-infinite binary array of optical waveguides, and revealed a link between the linear surface modes supported by the defects and nonlinear localized states in the defect-free semi-infinite structure. We have found families of both discrete surface solitons and nonlinear Tamm states and analyzed their stability.

This work has been supported by Fondecyt grants 1050193 and 7050173 in Chile, and by the Australian Research Council in Australia.

[1] Yu. S. Kivshar, F. Zhang, and S. Takeno, Physica D **119**, 125 (1998).
[2] K. G. Makris, S. Suntsov, D. N. Christodoulides, G. I. Stegeman, and A. Hache, Opt. Lett. **30**, 2466 (2005).
[3] S. Suntsov, K. G. Makris, D. N. Christodoulides, G. I. Stegeman, A. Hache, R. Morandotti, H. Yang, G. Salamo, and M. Sorel, Phys. Rev. Lett. **96**, 063901 (2006).
[4] M. Molina, R. Vicencio, and Yu. S. Kivshar, Opt. Lett. **31** (2006), in press.
[5] I. E. Tamm, Z. Phys. **76**, 849 (1932).
[6] P. Yeh, A. Yariv, and A. Y. Cho, Appl. Phys. Lett. **32**, 104 (1978).
[7] Y. V. Kartashov, V. A. Vysloukh, and L. Torner, Phys. Rev. Lett. **96**, 073901 (2006).
[8] C. R. Rosberg, D. N. Neshev, W. Krolikowski, Yu. S. Kivshar, A. Mitchell, R. A. Vicencio, and M. I. Molina, arXiv physics/0603202 (2006).
[9] A. A. Sukhorukov and Yu. S. Kivshar, Opt. Lett. **27**, 2112 (2002).
[10] A. A. Sukhorukov and Yu. S. Kivshar, Opt. Lett. **28**, 2345 (2003).
[11] R. Morandotti, D. Mandelik, Y. Silberberg, J. S. Aitchison, M. Sorel, D. N. Christodoulides, A. A. Sukhorukov, and Yu. S. Kivshar, Opt. Lett. **29**, 2890 (2004).
[12] D. E. Pelinovsky, A. A. Sukhorukov, and Yu. S. Kivshar, Phys. Rev. E **70**, 036618 (2004).